

# Predictive model approach based direct power control for power quality conditioning

Houssam Eddine Medouce<sup>1</sup>  · Hocine Benalla<sup>1</sup>

Received: 22 December 2016 / Revised: 2 July 2017 / Published online: 22 October 2017

© The Society for Reliability Engineering, Quality and Operations Management (SREQOM), India and The Division of Operation and Maintenance, Lulea University of Technology, Sweden 2017

**Abstract** This paper has presented improved control structure based direct power control (DPC) applied for shunt active power filtering. Basically, DPC control strategy employs instantaneous active and reactive power terms as controlled variables. This work introduces an integration concept of predictive control algorithm for shunt active power filter system application. Process of this latter adopts discrete model of PWM converter in the aim to predict future behaviour of the system. Switching vector selection principles for predictive control is very different compared to conventional method. For conventional DPC the selection is performed via heuristic switching table while predictive DPC algorithm takes on an optimized way based on cost function minimization depending to power errors, this latter evaluate the effects of each active voltage vector and the one reducing the cost function is chosen to be applied in the next sampling period. The application of optimal switching state leads to regulate the input active and reactive power which resulted in the cancellation of harmonic power component contained in the network. Simulation results are presented to verify the validity and effectiveness of the proposed predictive DPC in terms of dynamic and steady state performance for shunt active power filtering application.

**Keywords** Direct power control · Harmonics · Predictive model based direct power control · Shunt active power filter (SAPF) · Non-linear load · Switching table · Cost function minimization

## 1 Introduction

The fast development in the field of manufacturing which we are living nowadays along with the well-being brought to humanity, as well there is a downside which is the contamination of electrical distribution networks accompanying this large scale development.

It is a key issue benefiting a good power quality for supply systems to ensure good function in convenient conditions for electrical equipments. Unfortunately wide spread use of non-linear charges in industry led to a significant degradation of power quality in the electrical distribution systems due of high harmonic currents generation. Therefore a lot of experts and researchers oriented to find solutions and to develop new techniques to address this new challenge.

Hence, in the literature various solutions were introduced to mitigate undesired harmonics as power filtering (passive, active, and hybrid) with numerous topologies (shunt, series) for two-wire single phase, three-wire three-phase and four-wire three-phase systems (Singh et al. 1999). These solutions have been implemented by using electrical passive elements or current and voltage source inverters to upgrade network power quality.

Though, passive filtering by second order filters solution involving many drawbacks such as aging, adjustment problems and resonance, and as well need to design one

---

✉ Houssam Eddine Medouce  
b.houssam19@hotmail.fr

Hocine Benalla  
benalladz@yahoo.fr

<sup>1</sup> Department of Electrical Engineering, Electrical Engineering Laboratory (LEC), Mentouri Brothers University, Constantine, Algeria

filter for every undesired harmonic frequency to be wiped out (Chaoui et al. 2007).

The development in power electronics technology and digital signal processing opened the way for the emergence of active power filters as a effective solution for harmonics currents and low power factor (Akagi 1996; Singh et al. 1999). The shunt active power filter (SAPF) has been introduced to eliminate complications accompanying the use of passive filters, hence SAPF systems knew significant attention since its release by Gyugyi (Gyugyi 1976). Practically found that harmonic mitigation via a shunt active power filter (SAPF) more efficient and more flexible compared to a passive power filter (Izhar et al. 2004; Routimo et al. 2007). The efficiency of the SAPF depends mainly on the topology of voltage source inverter and type of extraction algorithm which used to provide reference signals (current or power) and as well the applied control approach for the filtering system.

The SAPF has excellent compensation capability permits simultaneous suppression of harmonic currents and compensation of the reactive power. For this purpose, the main goal of SAPF control process is to generate compensation current that is equal to the harmonic current contents.

In this context, and as pointed out by Soares et al. (2000), majority of active filters use the current control approach in a cascaded multi-loop control structure. Harmonics and reactive power are compensated by the inner current control loop, and the outer voltage control loop regulates the dc link voltage. Due to the dynamic response rapidity of the inner current control loop compared to output voltage control loop then it is necessary using a capacitor with sufficient storage capability in order to avoid overshoot of dc link voltage in transient conditions and maintained constant. Several control methods are proposed and reported in the literature such as proportional-integral (PI) control and hysteresis control (Buso et al. 1998), dead-beat control (Malesani et al. 1998), repetitive-based control (Mattavelli et al. 2001), adaptive control (Shyu et al. 2008), and nonlinear control (Rahmani et al. 2010). Due to the quick development of micro-processing technology, many control methods based current controller are developed including of a proportional controller plus multiple sinusoidal signal integrators (Rahmani et al. 2010), a PI controller plus a series of resonant controllers (Lascu et al. 2009; Limongi et al. 2009), or vector PI (VPI) controllers (Lascu et al. 2007).

The control of SAPF based current suffers from several drawbacks such as steady state error and band width limitation. In order to overcome drawbacks introduced by the current controllers an efficient control is proposed for three phase PWM converters called direct power control DPC by Noguchi et al. (1998). Advantages of this control method

presents in fast dynamic response and simplicity of implementation compared to other strategies. DPC control strategy is developed analogously with the well-known direct torque control (DTC) used for adjustable speed drives (Takahashi and Nogushi 1986). The controlled variables for DPC method are active and reactive powers while DTC method regulates flux and torque terms. The most important features of DPC control are lack of closed current loops and the direct selection of optimal switching state from a heuristic switching table based on dual variable criterion. The dual variable criterion consists digitized signals of power errors and grid voltage position.

Emergence of conventional DPC usage for SAPF systems is introduced by (Chaoui et al. 2008; Chen and Joos 2008). Furthermore, a modified DPC applied for an SAPF system is proposed by (Mesbahi et al. 2014; Djazia et al. 2015) in order to remedy adverse effects created by unbalance and distorted grid voltage conditions. As well, multifunctional SAPF system based DPC for a photovoltaic generator is presented by Boukezata et al. (2016).

Research paper proposed by Cortes et al. (2008) introduced a predictive DPC control for PWM rectifiers. This latter is conducted by the evaluation of the effect of each vector among finite set of possible switching states in the aim to minimize power errors. The switching state that produces the minimum variation for power errors is opted and applied during the next sampling period.

As knowledge gap and main contribution, in this paper we incorporate and benefit concept and merits offered by the predictive DPC control to improve steady state operation of a three phase SAPF system.

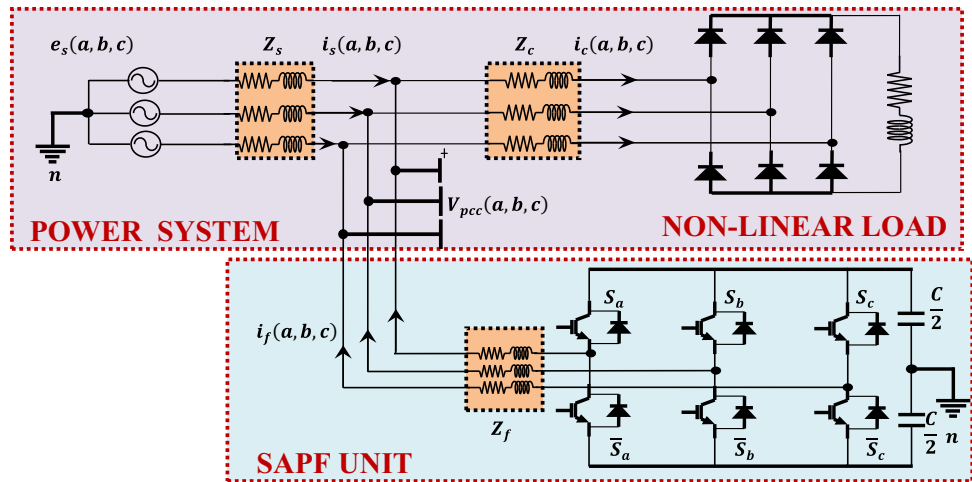
This paper is organized as follows. In Sect. 2 description and modeling and function principle analysis of the studied system. In Sect. 3 basics and mathematical background of conventional and predictive DPC are outlined. In Sect. 4 proposed control scheme is tested in terms of validity and effectiveness and a comparative study between conventional and proposed DPC is carried out.

## 2 Topology description and modelling of SAPF system

### 2.1 Topology description of SAPF system

The role of SAPF is the cancelation of current harmonics in the distribution networks by injecting compensating current at the point of common coupling (PCC) which characterizes with the same magnitude and phase compared to the harmonic current drawn by the nonlinear loads to achieve sinusoidal waveform for line currents. The fundamental structure block of the SAPF is shown in Fig. 1. The SAPF system is consisted of standard three-phase IGBT based

**Fig. 1** System based shunt active power filter (SAPF) unit



voltage source inverter (VSI) bridge with the input impedance ( $Z_f$ ) and a dc bus capacitor ( $C$ ) has ability managing sudden transients. A three-phase ac grid with line impedance ( $Z_s$ ) is supplying power for an non-linear load constituted of uncontrolled three-phase rectifier based diodes with a resistive-inductive load (Mesbahi et al. 2014).

**2.2 SAPF modelling**

Detailed knowledge about the structure and operation mechanism of SAPF is very important to be able to provide accurate mathematical model. The SAPF composed from an ideal two level three phase voltage source inverter which consists three branches ( $a, b, c$ ) with two switches in each one. The switch state in the  $x$ th branch has two possible states  $S_x = 1$  (closed switch) or  $S_x = 0$  (opened switch).

The three phase voltage system assumed balanced and pure sinusoidal waveform:

$$\begin{cases} e_{sa}(t) = V_m \sin(\omega t) \\ e_{sb}(t) = V_m \sin\left(\omega t - \frac{2\pi}{3}\right) \\ e_{sc}(t) = V_m \sin\left(\omega t - \frac{4\pi}{3}\right) \end{cases} \quad (1)$$

$V_m$  is the magnitude of simple phase voltage and  $\omega$  is the angular frequency of the grid.

As already reported supply network is symmetrical and balanced then some assumptions are taking into account:

$$\begin{cases} e_{sa} + e_{sb} + e_{sc} = 0 \\ i_{sa} + i_{sb} + i_{sc} = 0 \\ i_{la} + i_{lb} + i_{lc} = 0 \\ i_{fa} + i_{fb} + i_{fc} = 0 \end{cases} \quad (2)$$

As depicted in Fig. 2 a simplified phase circuit for the system is presented. It consists of power grid ( $e_s$ ) connected with PCC point through source impedance  $Z_s$  and non-

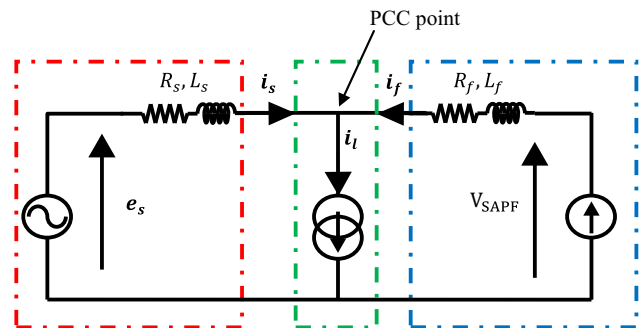


**Fig. 2** Equivalent circuit of SAPF system (Mesbahi et al. 2014)

linear load absorbs pure distorted current  $i_l$  and SAPF which represents the association between voltage source inverter and filter impedance  $Z_f$ .

By ignoring effect of source impedance the relationship which links network and SAPF unit can be expressed in the following simplified formulation:

$$V_{SAPF} = e_s - L_f \frac{di_f}{dt} - R_f i_f \quad (3)$$

where  $V_{SAPF}$  the output voltage provided by the SAPF while is the grid voltage.

As already mentioned the grid power considered symmetrical and balanced and by application of Kirchhoff law on the simplified phase circuit of SAPF in Fig. 2. Then a detailed expression of Eq. 3 can be rewritten in the following equation pattern:

$$\begin{aligned} V_{SAPF}^a &= e_{sa} - L_f \frac{di_{fa}}{dt} - R_f i_{fa} = S_a V_{dc} - V_{nk} \\ V_{SAPF}^b &= e_{sb} - L_f \frac{di_{fb}}{dt} - R_f i_{fb} = S_b V_{dc} - V_{nk} \\ V_{SAPF}^c &= e_{sc} - L_f \frac{di_{fc}}{dt} - R_f i_{fc} = S_c V_{dc} - V_{nk} \\ C \frac{dV_{dc}}{dt} &= S_a i_{fa} + S_b i_{fb} + S_c i_{fc} \end{aligned} \quad (4)$$

The sum of the first three equations in Eq. 4 leads to:

$$\begin{cases} V_{SAPF}^a + V_{SAPF}^b + V_{SAPF}^c = 0 \\ V_{nk} = \frac{S_a + S_b + S_c}{3} V_{dc} \end{cases} \quad (5)$$

Substituting Eq. 5 in Eq. 4 yields

$$\begin{aligned} \frac{di_{fa}}{dt} &= -\frac{R_f}{L_f} i_{fa} - \frac{V_{dc}}{L_f} \left( S_a - \frac{S_a + S_b + S_c}{3} \right) + \frac{1}{L_f} e_{sa} \\ \frac{di_{fb}}{dt} &= -\frac{R_f}{L_f} i_{fb} - \frac{V_{dc}}{L_f} \left( S_b - \frac{S_a + S_b + S_c}{3} \right) + \frac{1}{L_f} e_{sb} \\ \frac{di_{fc}}{dt} &= -\frac{R_f}{L_f} i_{fc} - \frac{V_{dc}}{L_f} \left( S_c - \frac{S_a + S_b + S_c}{3} \right) + \frac{1}{L_f} e_{sc} \end{aligned} \quad (6)$$

Can summarize control signals as follow:

$$\begin{cases} q_a = S_a - \frac{S_a + S_b + S_c}{3} \\ q_b = S_b - \frac{S_a + S_b + S_c}{3} \\ q_c = S_c - \frac{S_a + S_b + S_c}{3} \end{cases} \quad (7)$$

$$q_{abc} = K S_{abc}$$

With:  $q_{abc} = [q_a q_b q_c]^T$ ;  $S_{abc} = [S_a S_b S_c]^T$  and

$$K = \frac{1}{3} \begin{bmatrix} 2 & -1 & -1 \\ -1 & 2 & -1 \\ -1 & -1 & 2 \end{bmatrix}$$

According to instantaneous reactive power theory proposed by Akagi (1996) an algebraic transformation (Concordia transformation) for grid voltages and currents from  $(a, b, c)$  to  $(\alpha, \beta)$  coordinates is performed.

$$\begin{bmatrix} e_s^\alpha \\ e_s^\beta \end{bmatrix} = \sqrt{\frac{2}{3}} \begin{bmatrix} 1 & -\frac{1}{2} & -\frac{1}{2} \\ 0 & \frac{\sqrt{3}}{2} & -\frac{\sqrt{3}}{2} \end{bmatrix} \begin{bmatrix} e_{sa} \\ e_{sb} \\ e_{sc} \end{bmatrix} \quad (8)$$

$$\begin{bmatrix} i_s^\alpha \\ i_s^\beta \end{bmatrix} = \sqrt{\frac{2}{3}} \begin{bmatrix} 1 & -\frac{1}{2} & -\frac{1}{2} \\ 0 & \frac{\sqrt{3}}{2} & -\frac{\sqrt{3}}{2} \end{bmatrix} \begin{bmatrix} i_{sa} \\ i_{sb} \\ i_{sc} \end{bmatrix} \quad (9)$$

Instantaneous active and reactive power of the grid can be written as follow:

$$\begin{bmatrix} P_s \\ Q_s \end{bmatrix} = \begin{bmatrix} e_s^\alpha & e_s^\beta \\ -e_s^\beta & e_s^\alpha \end{bmatrix} \begin{bmatrix} i_s^\alpha \\ i_s^\beta \end{bmatrix} \quad (10)$$

### 2.3 SAPF function principle

Shunt active power filter (SAPF) can be considered as a controlled current source has ability to generate the suitable compensating current which must be corresponding to load current harmonic content drawn by non-linear loads.

In order to provide a reference system based on power quantities then instantaneous power balance between power transmitted by grid and SAPF unit and power drawn by load have to be investigated.

As shown in Fig. 3, it is considered that  $(P_s, Q_s)$  are respectively active and reactive powers delivered by the grid,  $(P_f, Q_f)$  are respectively active and reactive powers injected by the filter and  $(P_l, Q_l)$  are respectively active and reactive consumed powers by non-linear load. The role of SAPF is to compensate reactive power and to address problem of harmonic currents in the grid side. This aim is possible to achieve by the regulation of grid side active power to be equal to the continuous component (fundamental part) of load power ( $P_s = \bar{P}_l$ ) and as well grid side reactive power equal to zero ( $Q_s = 0$ ). In order to impose this condition on the system then it is necessary that harmonic power component and reactive power in load side be fully fed by SAPF unit. So the power balance of the system can be written in the following form:

$$\begin{cases} P_s = \bar{P}_l \\ Q_s = 0 \end{cases} \quad (11)$$

$$\begin{cases} P_f = P_l - P_s = P_l - \bar{P}_l = \tilde{P}_l \\ Q_f = Q_l - Q_s = Q_l \end{cases} \quad (12)$$

## 3 Control of SAPF

### 3.1 Conventional direct power control (DPC)

As shown in Fig. 4 overview on the control scheme based conventional DPC is presented. The three-phase ac voltages and currents of the network are measured and transformed into the stationary  $\alpha - \beta$  reference frame. The active and reactive powers are calculated according to Eq. 10.

The grid voltage position is estimated by using phase locked loop block (PLL) or by a simple trigonometric function as given in Eq. 16. The calculated active and reactive  $P_s, Q_s$  power are compared to their references values  $P_s^*, Q_s^*$  respectively in order to generate digitized power error signals  $S_P$  and  $S_Q$ .

The selection of optimal switching state is performed via predefined switching table. The accuracy of selection requires the accurate calculation of digitized power error signals and grid voltage angular position.

#### 3.1.1 Digitized signals of power errors

Instantaneous active and reactive power variation over a given reference is very important for the process of optimal vector selection.

**Fig. 3** Power flow in the SAPF system

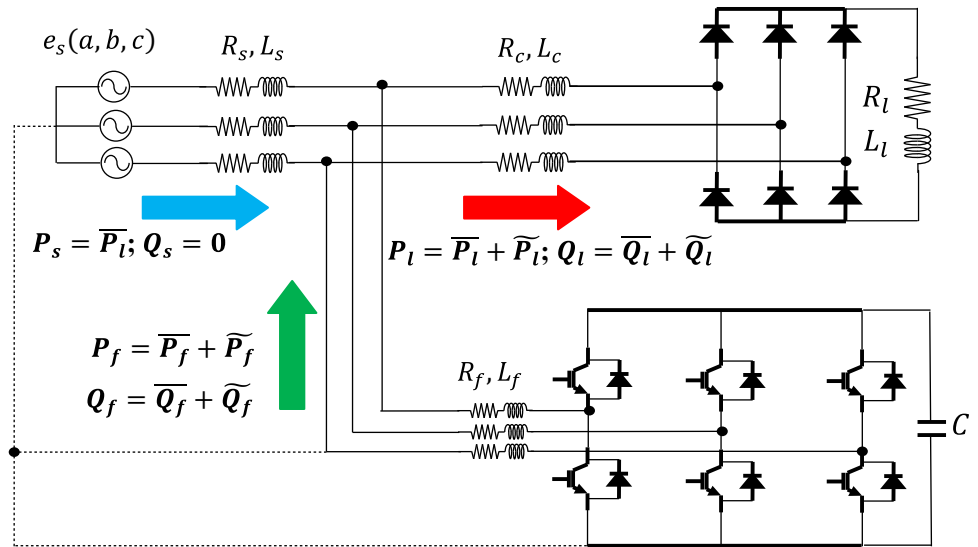
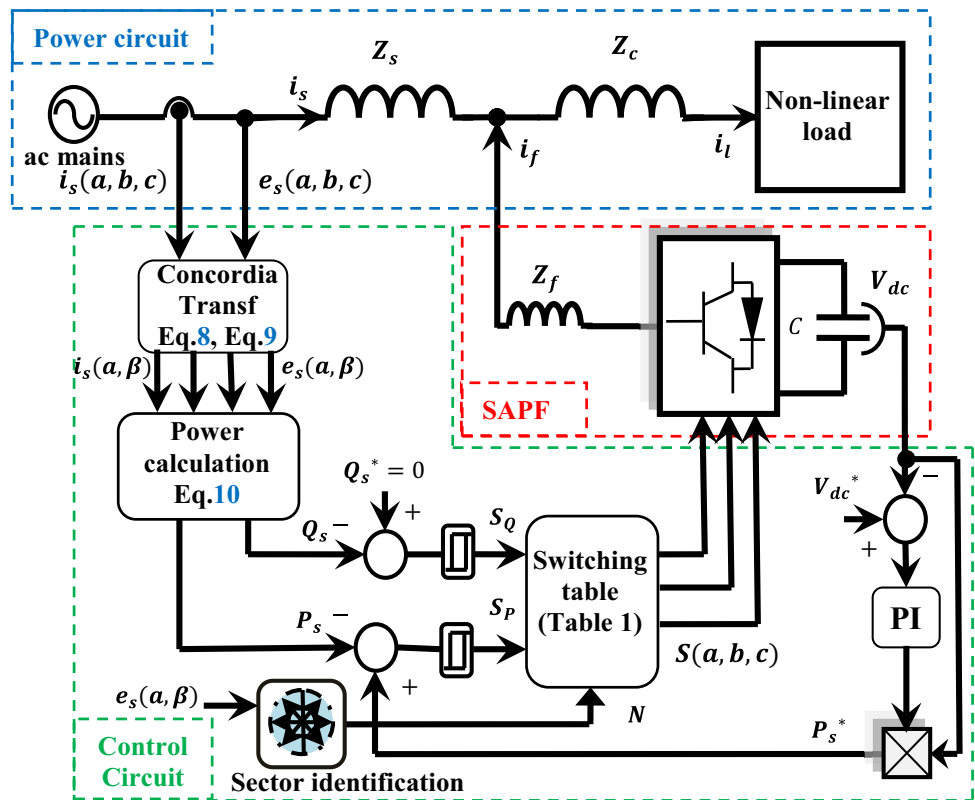


**Fig. 4** Conventional direct power control block diagram



$$\begin{cases} \Delta P_s = P_s^* - P_s \\ \Delta Q_s = Q_s^* - Q_s \end{cases} \quad (13)$$

The DPC controller needs to use the power error signal in a digitized form and it is possible to obtain by using two level hysteresis comparators.

$$\begin{cases} S_p = 1 & \text{if } P_s^* - P_s \geq h_p \\ S_p = 0 & \text{if } P_s^* - P_s \leq -h_p \end{cases}$$

$$\begin{cases} S_q = 1 & \text{if } Q_s^* - Q_s \geq h_q \\ S_q = 0 & \text{if } Q_s^* - Q_s \leq -h_q \end{cases} \quad (14)$$

$h_p, h_q$  are hysteresis bands.

### 3.1.2 Grid voltage angular position identification

Angular position of grid voltage is required in digitized data form in order to fulfil the control process hence the

$(\alpha, \beta)$  plan is divided into twelve sectors as depicted in Fig. 5.

$$(n - 2) \frac{\pi}{6} \leq \theta \leq (n - 1) \frac{\pi}{6}, \quad n = 1, 2, \dots, 12. \quad (15)$$

The angular position can be calculated with the following equation:

$$\theta = \arctg \left( \frac{e_{s\beta}}{e_{s\alpha}} \right) \quad (16)$$

### 3.1.3 Switching table synthesizing

Application of any one out of the set of possible eight switching vectors ( $V_0$ – $V_7$ ) for the power converter, leads to make specified variation amount for the grid instantaneous power. The influence of each vector can be outline in two main effects on power converter which are capacitive (power source) or inductive effect (load) (Figs. 6, 7). The optimal switching states are summarized in Table 1.

## 3.2 Direct power control based predictive approach

In order to maintain power balance mentioned in Eqs. 11 and 12 then, predictive control concept based DPC is applied for the SAPF system. Similarly as conventional DPC also predictive DPC considers active and reactive grid power as controlled variables.

Predictive DPC control strategy is executed basically through the following two steps:

### 3.2.1 Generation of the predictive model

In Order to simplify the modelization we are adopted the dynamic equation of grid current in the vector form.

$$L_s \frac{di_s}{dt} = e_s - V_{SAPF} - R_s i_s \quad (17)$$

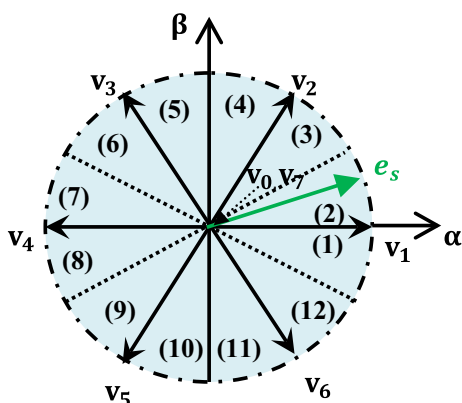


Fig. 5 Angular position of grid voltage vector

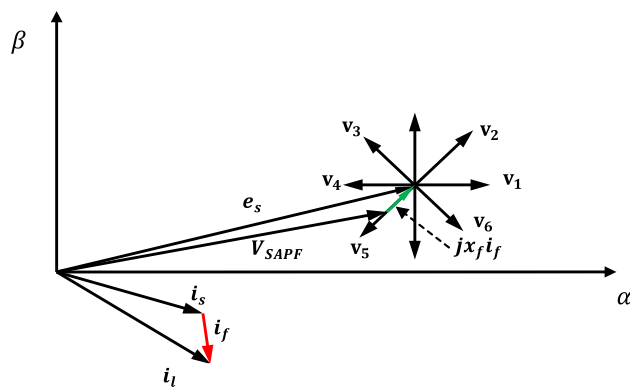


Fig. 6 Influence of switching states on vector diagram of SAPF system

The discretization act is done by approximating the derivative operation as variation over one sampling period.

$$\frac{di_s}{dt} \approx \frac{i_s(k + 1) - i_s(k)}{T_s} \quad (18)$$

By substituting Eq. 18 in Eq. 17 then predicted current model is provided:

$$i_s(k + 1) = \left( 1 - \frac{R_s T_s}{L_s} \right) i_s(k) + \frac{T_s}{L_s} [e_s(k) - V_{SAPF}(k)] \quad (19)$$

where  $i_s(k + 1)$  is the predicted grid current vector at  $k + 1$  instant, for a given voltage vector generated by SAPF.

Then the predicted active and reactive power terms can be expressed in the following form:

$$\begin{cases} P_s(k + 1) = Re[e_s(k + 1)i_s(k + 1)^*] \\ Q_s(k + 1) = Im[e_s(k + 1)i_s(k + 1)^*] \end{cases} \quad (20)$$

\* represents conjugate operator. *Re* represents the real component of the vector. *Im* represents the imaginary component of the vector.

The predicted input grid voltage  $e_s(k + 1)$  after one sampling time period  $T_s$ .

$$e_s(k + 1) = e_s(k)e^{i\Delta\theta} \quad (21)$$

where  $\Delta\theta = \omega T_s$  is the angle of forward progression with angular velocity  $\omega$  of the grid voltage vector during one sampling period.

Can assume that grid voltage is constant over two successive periods by considering that sampling time period  $T_s$  is small enough.

Hence, Eq. 20 can be simplified as follow:

$$\begin{cases} P_s(k + 1) = Re[e_s(k)i_s(k + 1)^*] \\ Q_s(k + 1) = Im[e_s(k)i_s(k + 1)^*] \end{cases} \quad (22)$$

**Fig. 7** Predictive direct power control block diagram

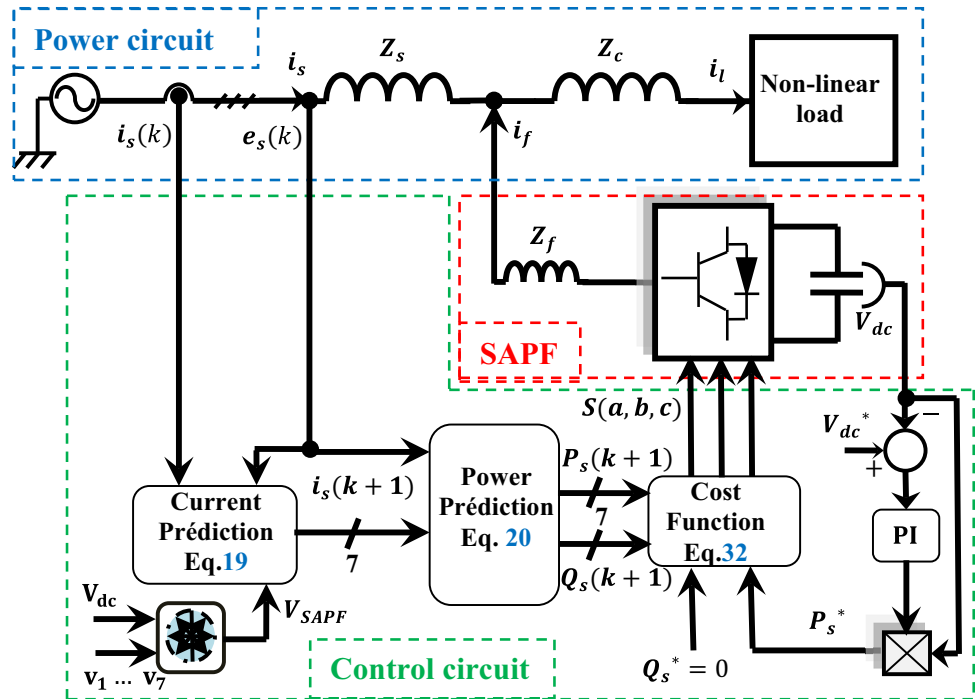


**Table 1** Switching table

$S_p$	$S_Q$	1	2	3	4	5	6	7	8	9	10	11	12
0	0	V <sub>6</sub>	V <sub>1</sub>	V <sub>1</sub>	V <sub>2</sub>	V <sub>2</sub>	V <sub>3</sub>	V <sub>3</sub>	V <sub>4</sub>	V <sub>4</sub>	V <sub>5</sub>	V <sub>5</sub>	V <sub>6</sub>
0	1	V <sub>1</sub>	V <sub>2</sub>	V <sub>2</sub>	V <sub>3</sub>	V <sub>3</sub>	V <sub>4</sub>	V <sub>4</sub>	V <sub>5</sub>	V <sub>5</sub>	V <sub>6</sub>	V <sub>6</sub>	V <sub>1</sub>
1	0	V <sub>6</sub>	V <sub>7</sub>	V <sub>1</sub>	V <sub>0</sub>	V <sub>2</sub>	V <sub>7</sub>	V <sub>3</sub>	V <sub>0</sub>	V <sub>4</sub>	V <sub>7</sub>	V <sub>5</sub>	V <sub>0</sub>
1	1	V <sub>7</sub>	V <sub>7</sub>	V <sub>0</sub>	V <sub>0</sub>	V <sub>7</sub>	V <sub>7</sub>	V <sub>0</sub>	V <sub>0</sub>	V <sub>7</sub>	V <sub>7</sub>	V <sub>0</sub>	V <sub>0</sub>

As well, it is possible to express the predictive model in different way according to the complex power form.

Based on what was already reported by Zhang et al. (2013), the grid side complex power  $S_s$  expression can be calculated from grid voltage and current vectors as:

$$S_s = P_s + jQ_s = \frac{3}{2}(e_s i_s^*) \tag{23}$$

Based on Eq. 17 derivative expression of line current could be represented as follow:

$$\frac{di_s}{dt} = \frac{1}{L_s}[e_s - V_{SAPF} - R_s i_s] \tag{24}$$

As mentioned before it is considered that the grid is symmetrical and balanced. Therefore the voltage source can be expressed in the exponential form  $e_s = |e_s|e^{j\omega t}$ .

The derivative expression of line voltage is given by the following expression:

$$\frac{de_s}{dt} = \omega e_s \tag{25}$$

Substituting Eqs. 24 and 25 in Eq. 23 then derivative expression of complex power is given as:

$$\frac{dS_s}{dt} = \frac{1}{L_s} \left[ (|e_s|^2 - V_{SAPF}^* e_s) - (R_s i_s - j\omega L_s) S_s \right] \tag{26}$$

Slop terms of input active and reactive powers can be obtained by decomposing Eq. 26 into real and imaginary parts (Zhang et al. 2013).

$$\frac{dP_s}{dt} = \frac{3}{2L_s} \left[ (|e_s|^2 - Re[V_{SAPF}^* e_s]) \right] - \frac{R_s}{L_s} P_s - \omega Q_s \tag{27}$$

$$\frac{dQ_s}{dt} = \frac{3}{2L_s} Im(V_{SAPF}^* e_s) - \omega P_s + \frac{R_s}{L_s} Q_s \tag{28}$$

So it is possible to predict the behaviour of grid power in the next sampling period through the following predictive model:

$$P_s(k+1) = P_s(k) + \left[ \frac{3}{2L_s} \left[ (|e_s|^2 - Re[V_{SAPF}^* e_s]) \right] - \frac{R_s}{L_s} P_s - \omega Q_s \right] T_s \tag{29}$$

**Fig. 8** Selection of the optimal switching state

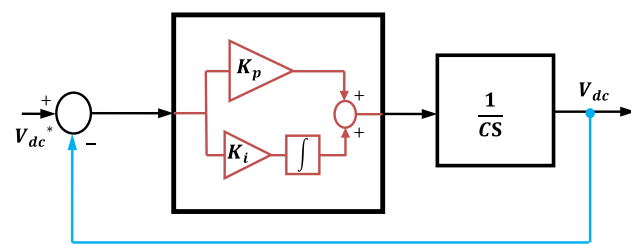
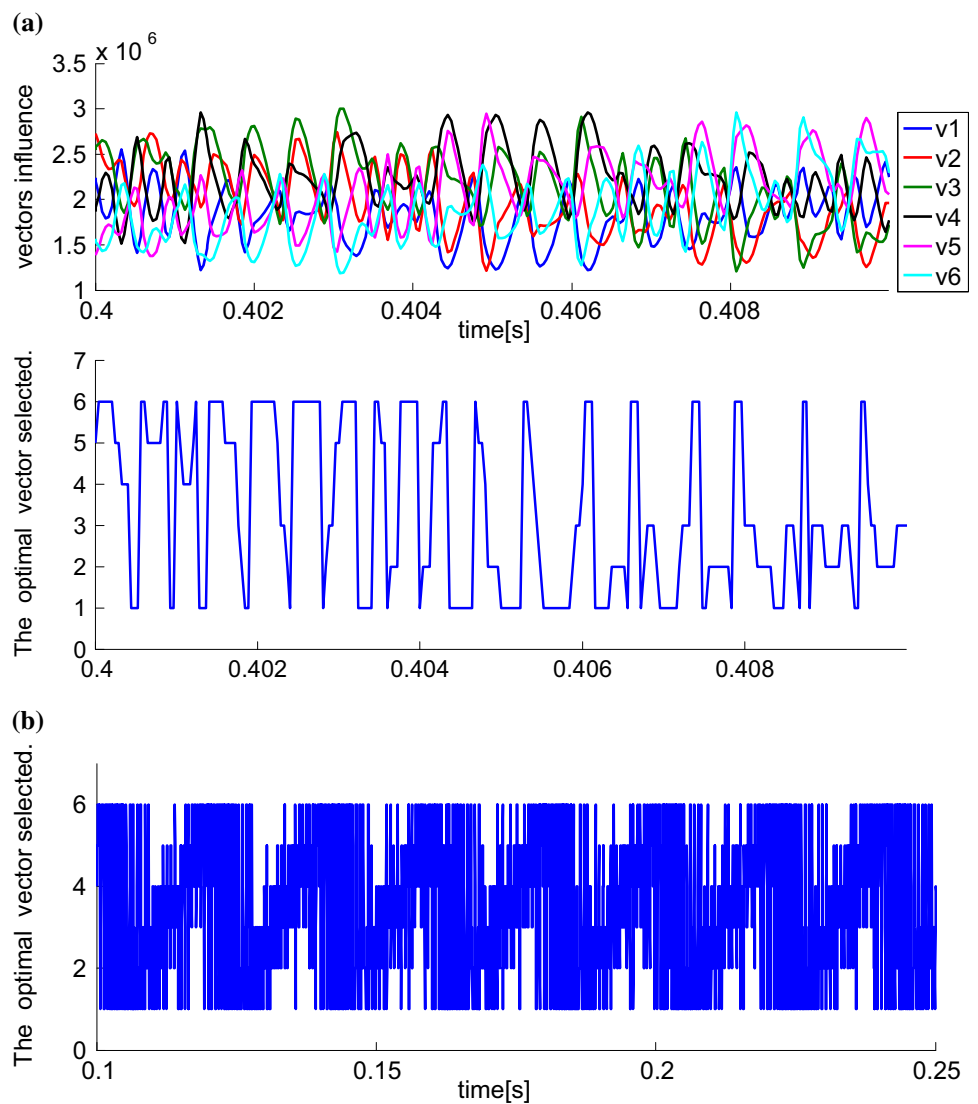


**Fig. 9** Block diagram of the dc bus voltage regulation loop

$$Q_s(k + 1) = Q_s(k) + \left[ \frac{3}{2L_s} \text{Im}(V_{SAPF}^* e_s) - \omega P_s + \frac{R_s}{L_s} Q_s \right] T_s \tag{30}$$

3.2.2 Selection of optimal vector via cost function

The main task for the proposed control technique is to establish the power balance reported in Eqs. 11 and 12

which represents the main condition to ensure efficient power filtration. Predictive control approach is used in order to drive the controlled variables to their respective references.

As depicted in Fig. 8 the basic idea of cost function is to evaluate effects of a set of switching vectors (six active vectors) at every sampling period. The decision about the optimal vector is done by the selection of the vector with low variation effect on cost function.

$$C_F = |Q_s^* - Q_s(k + 1)| + |P_s^* - P_s(k + 1)| \tag{31}$$

where  $P_s^*$  the reference value for grid active power which represent the output of dc link voltage controller and  $Q_s^*$  the reference value for grid reactive power which taken to be equal to zero in the aim to unify the power factor.

$$C_F = |Q_s(k + 1)| + |P_s^* - P_s(k + 1)| \tag{32}$$



**Fig. 10** Start up of SAPF in the case of conventional DPC  
**a** Line voltage phase-A (V).  
**b** Line current phase-A (A).  
**c** Filter current phase-A (A).  
**d** Capacitor voltage (V)

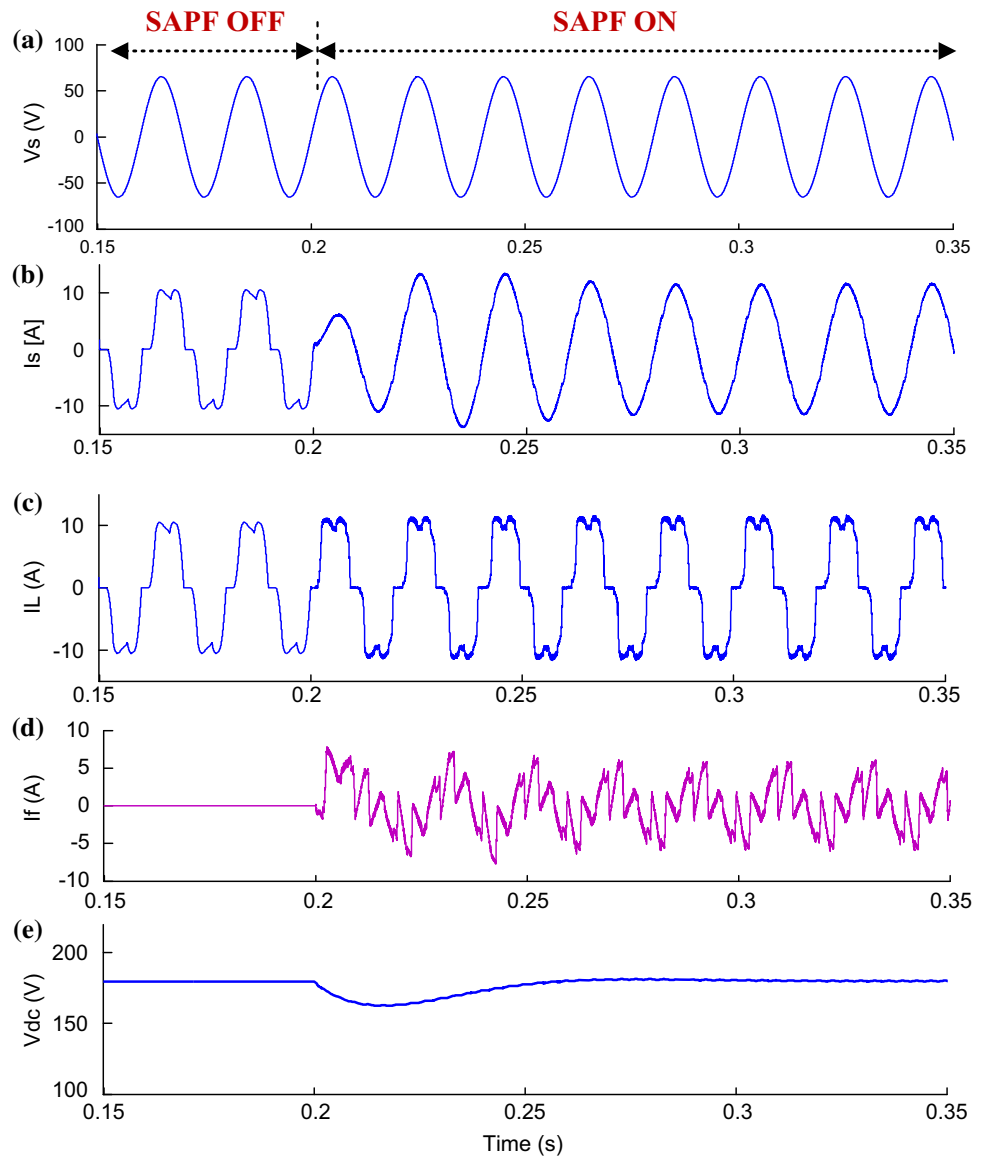


Figure 8 introduces the selection process of optimal switching vector which is depending on the level of variation occurred by each active vector on the cost function where the corresponding vector with low variation is chosen to be applied in the next sampling time period.

### 3.2.3 Dc link voltage regulation

Dc link voltage regulation depends mainly on the established power balance. For the stability of the system DC bus voltage must be constant in the steady state with limited variability during transients and start up. The dc bus voltage regulator can play the role of dynamic adapter in order to maintain the power balance between grid and load in the two following cases:

- $P_s > P_l$  the excessed power is drawn by the SAPF.
- $P_s < P_l$  the lacked power is fed by the SAPF.

Figure 9 shows block diagram of the dc link voltage regulator and detailed analysis of regulator parameters is given as:

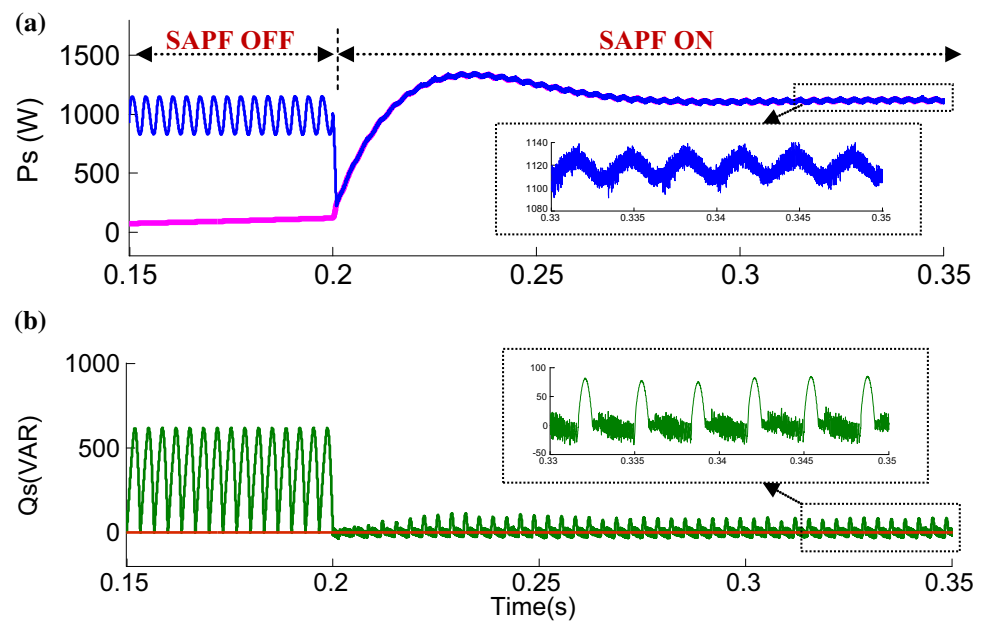
Based on the regulator structure depicted in Fig. 9 the identification of the transfer function with the general second order is defined as (Chaoui et al. 2008):

$$H(s) = \frac{2\xi\omega_n s + \omega_n^2}{s^2 + 2\xi\omega_n s + \omega_n^2} \tag{33}$$

Then parameters of capacitor voltage regulator can be expressed as

$$K_p = \frac{2\xi\omega_n}{\sqrt{2}V} \quad \text{and} \quad \tau_i = \frac{2\xi}{\omega_n} \quad \text{and} \quad K_i = \frac{1}{\tau_i} \tag{34}$$

**Fig. 11** Start up of SAPF in the case of conventional DPC  
**a** input active power (W),  
**b** input reactive power (VAR)



In order to compromise between dynamic performance and stability of the closed loop control it is recommended to choose:  $\xi = 0.707$  and  $f_n = \frac{\omega_n}{2\pi} = 50$  [Hz].

#### 4 Simulation results and discussion

The simulation of the system depicted in Fig. 1 is performed in the Matlab/SIMULINK environment. Data parameters used in the simulation process are listed in the “Appendix B”.

Results which have been presented in this section are the outcomes of the studied system for two control algorithms (conventional DPC and predictive DPC) under bellow cases:

**Case 1** analyse study of steady state operation with load value  $R_l = 10\Omega$  and capacitor voltage  $V_{dc} = 180V$ .

**Case 2:** analyse study of transient state operation with step load variation  $R_l = 10 \sim 20\Omega$ .

**Case 3:** analyse study of transient state operation with step capacitor voltage variation  $V_{dc} = 180 \sim 200 V$ .

For all simulation process it has been regarded the grid system as sinusoidal balanced network.

In order to highlight the superiority of the proposed control configuration a comparative study is carried out as a conclusion for this section.

**Case 1:** steady state operation.

SAPF unit is switched on at instant  $t = 0.2$  s.

Figures 10 and 12 show the source voltage ( $e_{sa}$ ), source current ( $i_{sa}$ ), load current ( $i_{la}$ ), filter current ( $i_{fa}$ ) and dc bus capacitor voltage ( $V_{dc}$ ) for both control strategies. The

instant the filter is switched on the source current turns quickly and gradually from the full distorted shape to the sinusoidal waveform which means effective attenuation of low order harmonic contents (5th, 7th, and 11th harmonics) induced due of non-linear load, as well capacitor voltage reaches a steady-state value around  $V_{dc} = 180V$  within a few mains periods (3 mains cycles). It is necessary to recall that capacitor is pre-charged in the aim to avoid start up divergence of input power and undesired overshoot for dc bus voltage.

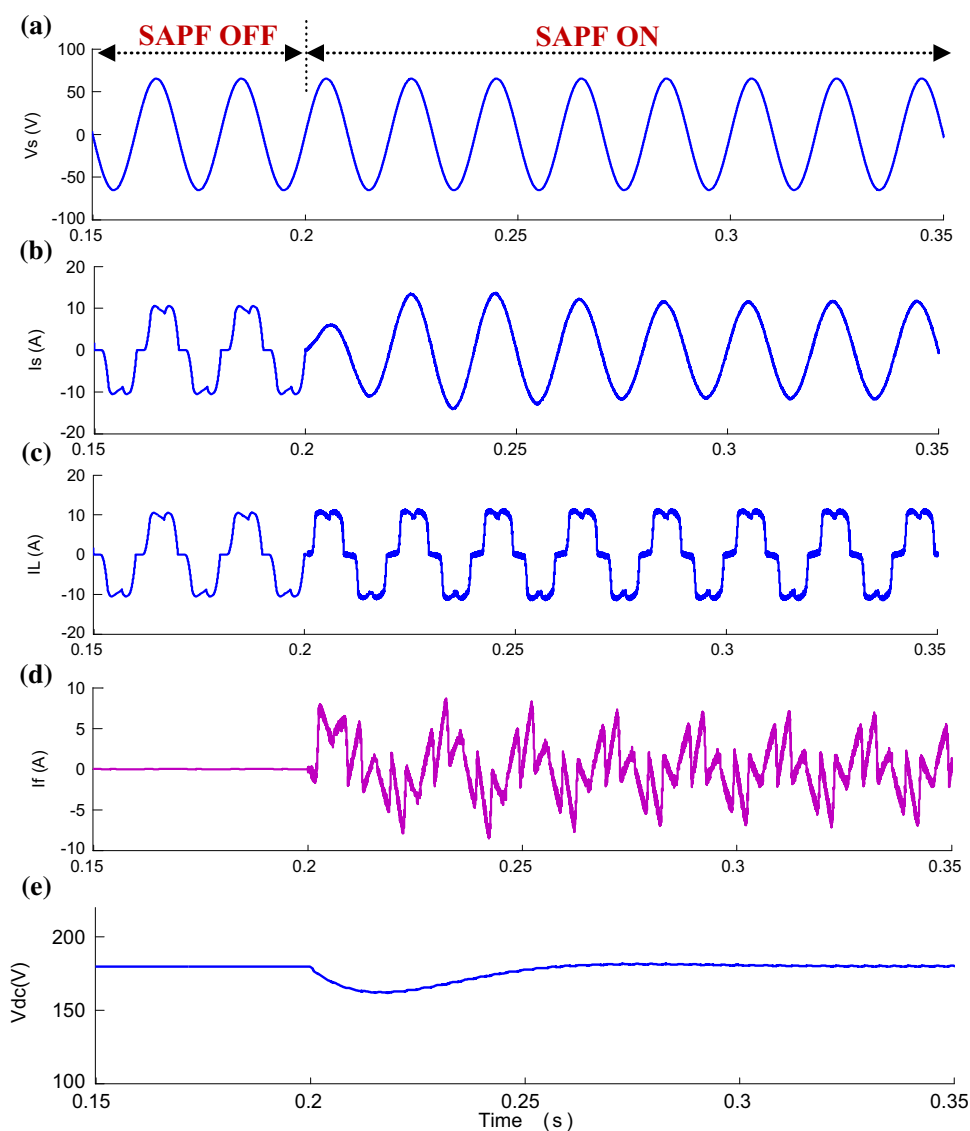
Figures 11 and 13 shows the input power evolution for both control strategies. We can observe that active power is achieved its rated value and reactive power regulated at zero level in the aim to ensure unity of power factor (Fig. 12).

**Case 2:** transient state operation with stepped resistor load from  $R_l = 10$  to  $20\Omega$  and fixed capacitor voltage  $V_{dc} = 180$ .

The resistor load is stepped at instant  $t = 0.5$  [s].

Figures 14 and 15 show various waveforms of source current ( $i_{sa}$ ), input active power ( $P_s$ ), input reactive power ( $Q_s$ ) and dc bus capacitor voltage ( $V_{dc}$ ) respectively for both control strategies. During resistor load change at instant 0.5 s can observe magnitude reduction of source current and active power delivered by grid and as well increasing in level of capacitor voltage which can be explained as dynamic power compensation ability for dc bus voltage regulator during transient conditions to maintain the power balance (mentioned in Sect. 3.2) at point of common coupling (PCC). In this case, excessed power delivered by grid is absorbed instantaneously by the

**Fig. 12** Start up of SAPF in the case of predictive DPC. **a** Line voltage phase-A (V). **b** Line current phase-A (A). **c** Filter current phase-A (A), **d** Capacitor voltage (V)



capacitor element which explains the slight and temporary rise in level of dc link voltage then the steady state of system can be restored within few cycles of time.

**Case 3** transient state operation with stepped capacitor voltage from  $V_{dc} = 180$  to  $200$  V and fixed resistor load  $R_l = 10 \Omega$ .

The capacitor voltage is stepped at instant  $t = 0.5$  s.

Figures 16 and 17 shows various waveforms of source current ( $i_{sa}$ ), input active power ( $P_s$ ), input reactive power ( $Q_s$ ) and dc bus capacitor voltage ( $V_{dc}$ ) for both control strategies. As can be seen variation of capacitor voltage has no effect on the level of generated power only temporary limited disturbance as transient perturbation. The capacitor voltage reaches its new level within 2 to 3 periods with low

overshoot which demonstrates satisfactory dynamic performance for dc bus voltage closed loop regulation.

#### 4.1 Comparative study

In order to prove effectiveness and superiority of the proposed control approach over the conventional one which is proposed by Chaoui et al. (2008), a comparative evaluation is done focused on key points such as:

- source current waveform,
- response time during start up and transient conditions,
- power ripple level and total harmonic distortion factor (THD).

As can be seen from previous results, during transient state operation in case of change of load or capacitor

**Fig. 13** Start up of SAPF in the case of predictive DPC **a** input active power (W), **b** input reactive power (VAR)

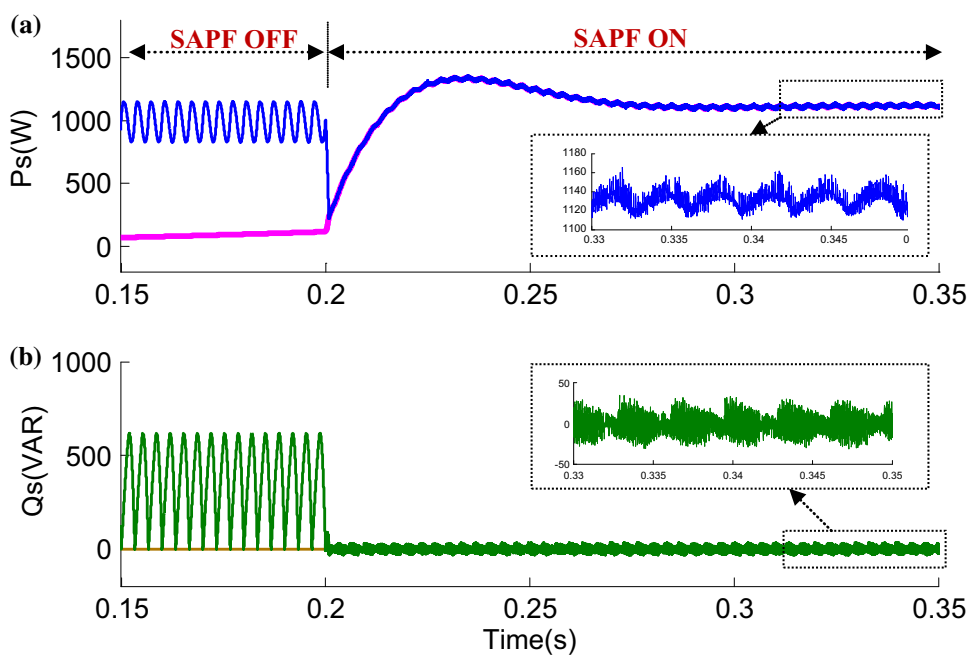


**Fig. 14** Load variation in case of conventional DPC. **a** Line current phase-A (A). **b** Input active power (W). **c** Input reactive power (VAR). **d** Capacitor voltage (V)

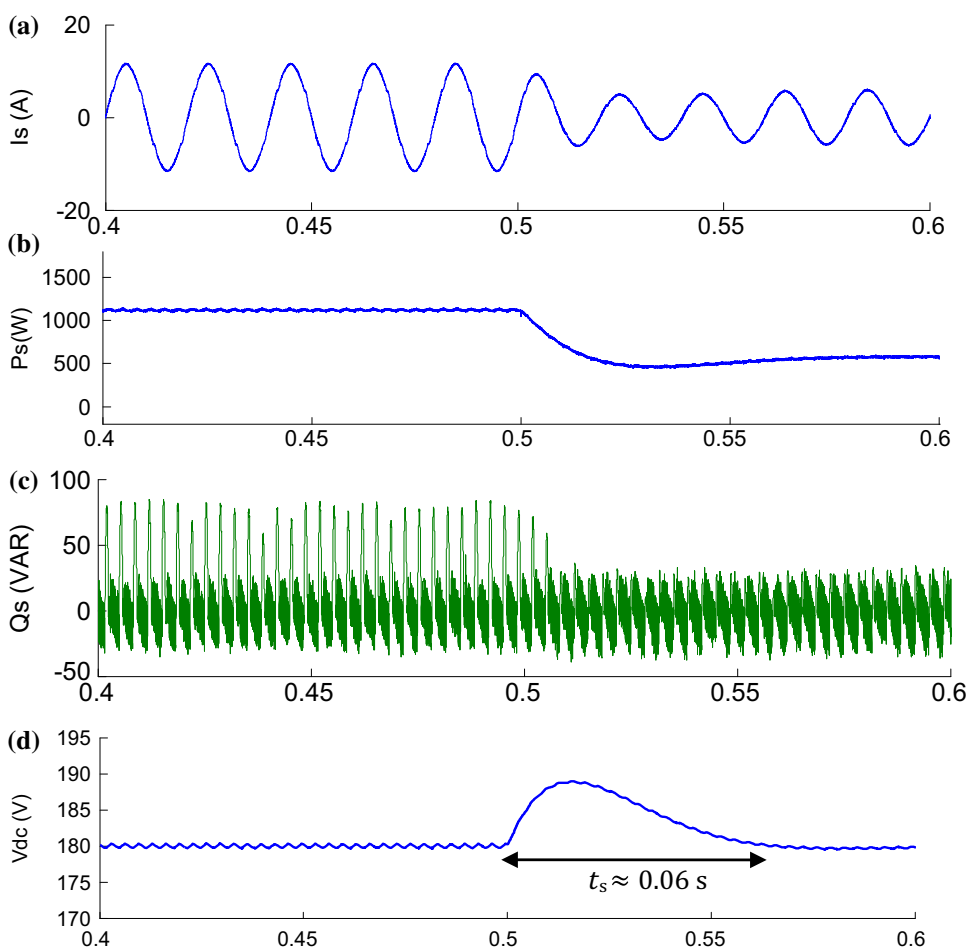
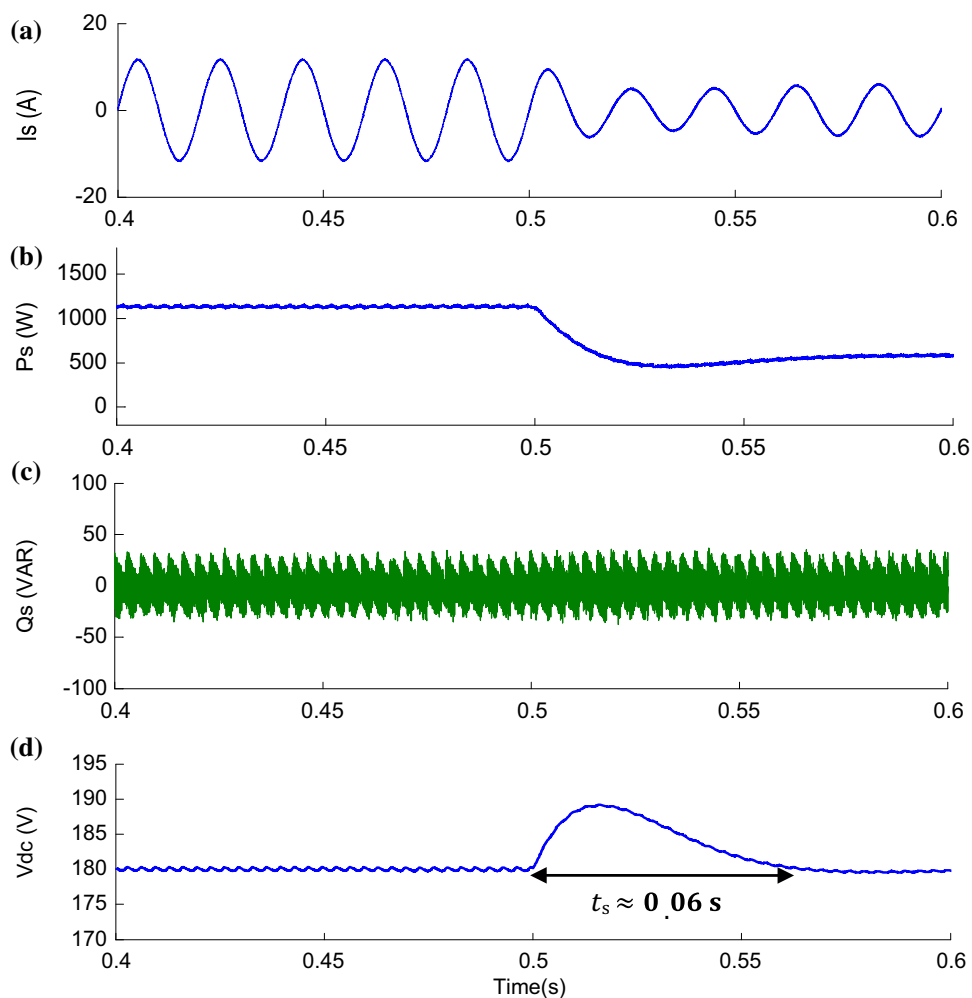


**Fig. 15** Load variation in case of predictive DPC. **a** Line current phase-A (A). **b** Input active power (W). **c** Input reactive power (VAR). **d** Capacitor voltage (V)



voltage the two control strategies converge to similar results, which means similarity of time response ( $t_s$ ) around 3 cycles of ac mains is achieved.

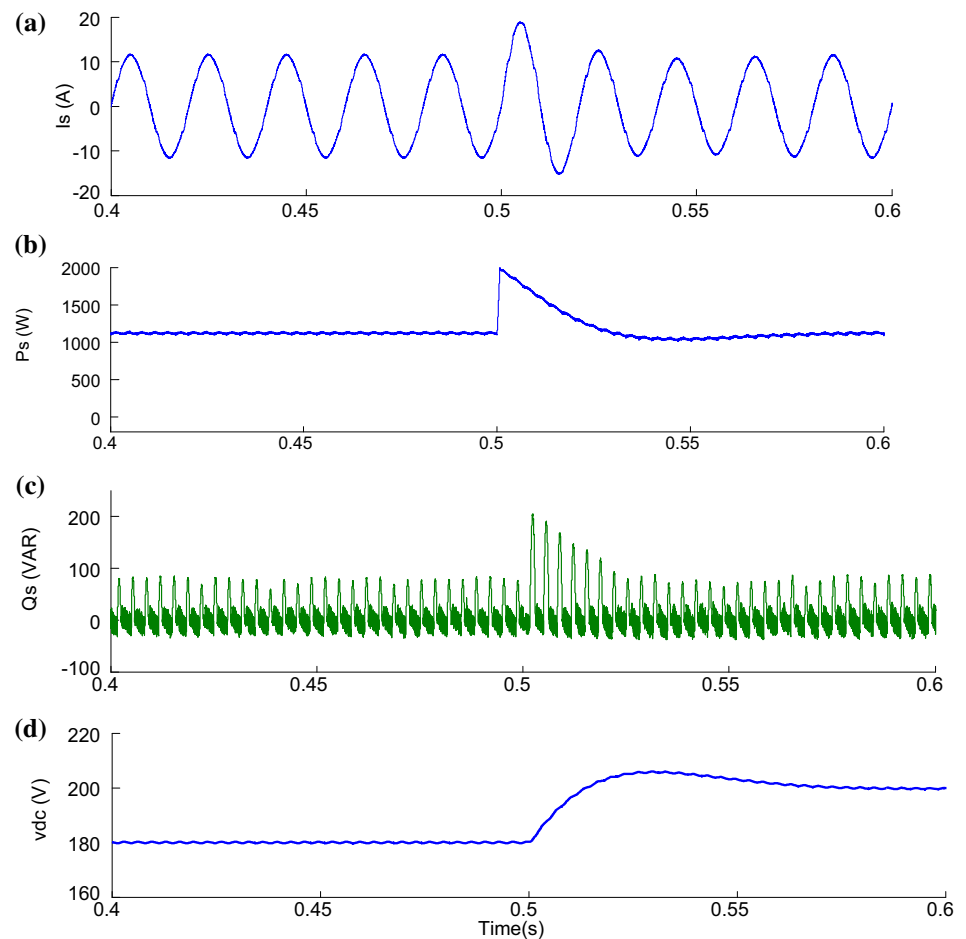
From Fig. 18 we can report two points the first one is that unity of power factor is satisfied by both control strategies and the second is a clear superiority for predictive DPC in terms of line current waveform where can observe a smooth sinusoidal waveform is established but on the other hand line current waveform in case of conventional DPC includes some distortion traces due of improper power regulation.

Figures 11 and 13 show the level of input power fluctuation in the steady state for both control strategies. Mentioned results demonstrate a clear superiority for predictive DPC over conventional one especially in terms of reactive power ripples.

For example the power ripple in conventional DPC case is around 100 VAR whereas for predictive DPC was restricted at level of 50 VAR.

Figure 19 presents the total harmonic distortion before and after the start up of SAPF for both control strategies. Presented results demonstrate that both control strategies

**Fig. 16** Transient impact of capacitor voltage variation in case of conventional DPC.  
**a** Line current phase-A (A).  
**b** Input active power (W).  
**c** Input reactive power (VAR).  
**d** Capacitor voltage (V)



has ability to drive source current below standard harmonic current limits (IEEE-519). The same results prove the superiority of proposed predictive DPC than conventional DPC in terms of THD with 1.42 and 2.88% respectively.

Briefly, both control strategies has similar performance and robustness for transient state operation but predictive DPC outperforms than conventional one with significant improvement for the steady state operation.

## 5 Conclusion

This paper has discussed integration of predictive DPC control for a shunt active power filter (SAPF) system. The concept of control approach is mainly based on the mathematical model of PWM converter to precalculate its behaviour for the next sampling cycle. Briefly, control process is done according to two phases, calculation of predicted power terms and an optimization act via a cost function minimization in order to select the optimal

switching states. The optimal switching states which selected every sampling time could to establish the desired power balance for the system; hence the suppression of harmonic power induced by non-linear loads in the grid side can be achieved successfully.

The numerical simulation is carried out in order to investigate the behaviour of system in steady and transient states for both control strategies. As wise findings, we can mention that predictive DPC control has been maintained main merits of conventional DPC such as perfect dynamic performance and lack of current closed loops and as well it has been offered significant improvement regarding to line current THD factor and power ripple in the steady state operation. A comparative study between proposed and conventional control techniques for SAPF application has been introduced. The obtained results were in accordance to the mathematical findings in previous sections and it has confirmed effectiveness and superiority of predictive DPC method over the conventional one.

**Fig. 17** Transient impact of capacitor voltage variation in case of predictive DPC. **a** Line current phase-A (A). **b** Input active power (W). **c** Input reactive power (VAR). **d** Capacitor voltage (V)

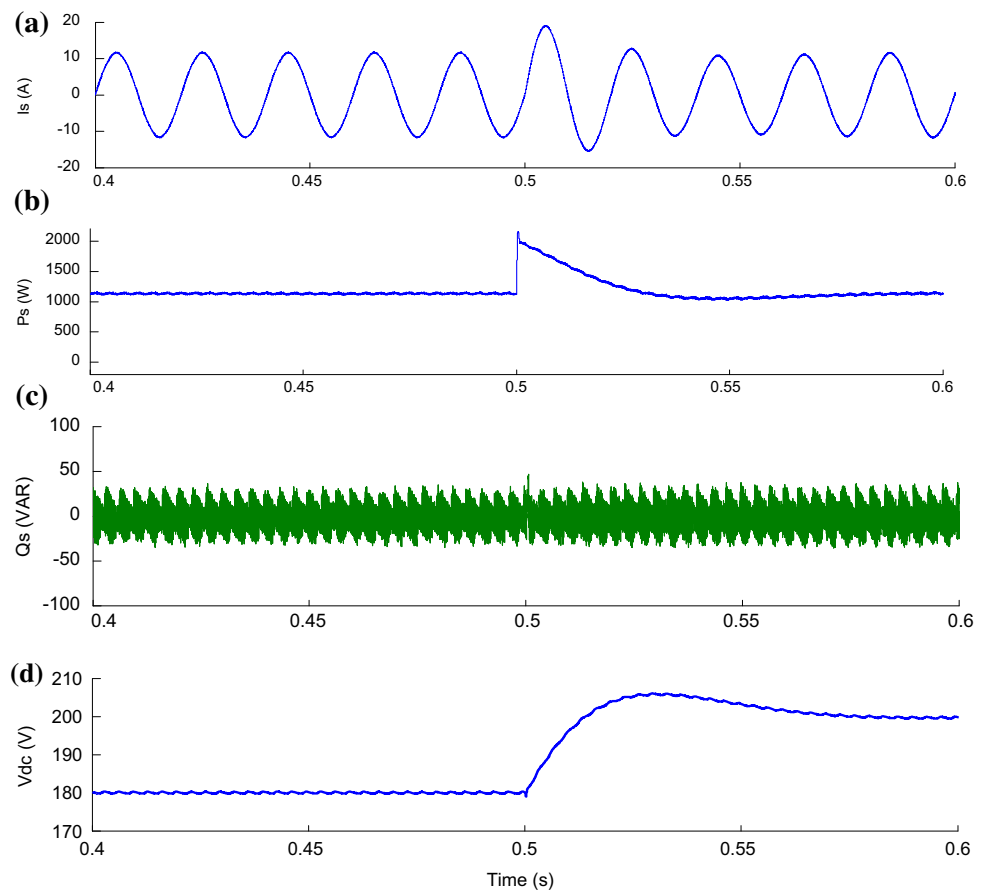


**Fig. 18** Line voltage (V) and current (A) for phase-A  
**a** conventional DPC  
**b** predictive DPC

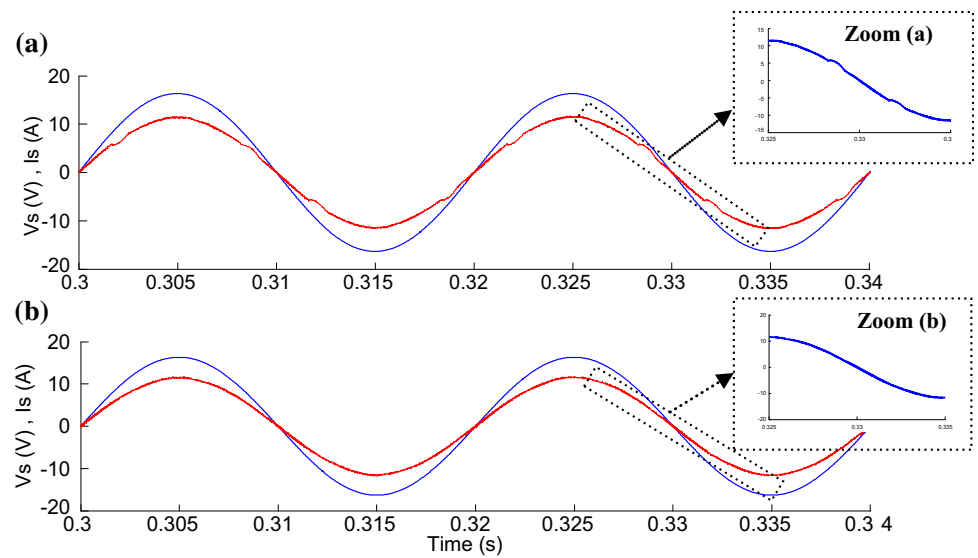
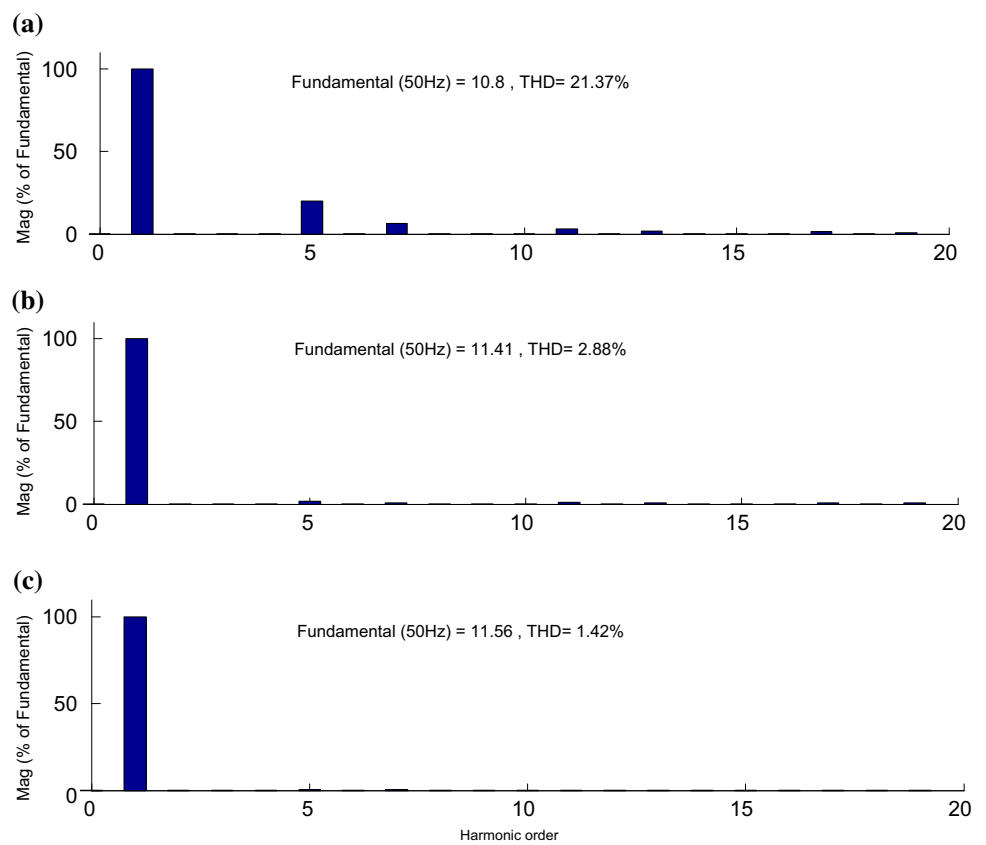


**Fig. 19** Harmonic spectrum of line current phase-A **a** before filtration **b** conventional DPC **c** predictive DPC



**Appendix A: Nomenclature**

$e_s(a, b, c)$	Source voltage of phase-A, phase-B and phase-C respectively
$V_{SAPF}(a, b, c)$	Inverter output voltage of phase-A, phase-B and phase-C respectively
$i_s(a, b, c)$	Source current of phase-A, phase-B and phase-C respectively
$i_l(a, b, c)$	Load current of phase-A, phase-B and phase-C respectively
$i_f(a, b, c)$	Filter current of phase-A, phase-B and phase-C respectively
$P_s$	Instantaneous grid active power
$P_s^*$	Command signal for grid active power
$Q_s$	Instantaneous grid reactive power
$Q_s^*$	Command signal for grid reactive power
–	Over the letter: continuous component
~	Over the letter: harmonic component
*	Over the letter: conjugate operator
$\alpha$	Direct component in the stationary reference frame
$\beta$	Quadratic component in the stationary reference frame

**Appendix B: Circuit parameters**

Circuit parameters	
$e_s$	Grid voltage 80 V
$R_s$	Grid filter resistor 0.1 $\Omega$
$L_s$	Grid filter inductor 2 mH
$R_c$	Load side filter resistor 0.01 $\Omega$
$L_c$	Load side filter inductor 0.5 mH
$R_f$	SAPF filter resistor 0.01 $\Omega$
$L_f$	SAPF filter inductor 1 mH
$R_l$	Load resistor 10 ~ 20 $\Omega$
$L_l$	Load inductor 1 mH
$C$	Capacitor 2200 $\mu$ F
$V_{dc}$	Dc link voltage 180 V



## References

- Akagi H (1996) New trends in active filters for power conditioning. *IEEE Trans Ind Appl* 32:1312–1322
- Boukezata B, Chaoui A, Gaubert J-P, Hachemi M (2016) Power quality improvement by an active power filter in grid-connected photovoltaic systems with optimized direct power control strategy. *Electr Power Compon Syst* 44:2036–2047
- Buso S, Malesani L, Mattavelli P (1998) Comparison of current control techniques for active filter applications. *IEEE Trans Ind Electron* 45:722–729
- Chaoui A, Gaubert JP, Krim F, Champenois G (2007) PI controlled three-phase shunt active power filter for power quality improvement. *Electr Power Compon Syst* 35:1331–1344
- Chaoui A, Krim F, Gaubert J-P, Rambault L (2008) DPC controlled three-phase active filter for power quality improvement. *Int J Electr Power Energy Syst* 30:476–485
- Chen BS, Joos G (2008) Direct power control of active filters with averaged switching frequency regulation. *IEEE Trans Power Electron* 23:2729–2737
- Cortes P, Rodríguez J, Antoniewicz P, Kazmierkowski M (2008) Direct power control of an AFE using predictive control. *IEEE Trans Power Electron* 23:2516–2523
- Djazia K, Krim F, Chaoui A, Sarra M (2015) Active power filtering using the zdpc method under unbalanced and distorted grid voltage conditions. *Energies* 8:1584–1605
- Gyugyi L (1976) Active ac power filters, in: *IEEE/IAS Annual Meeting*, 1976
- IzharM, Hadzer CM, Syafrudin M, Taib S, Idris S (2004) Performance for passive and active power filter in reducing harmonics in the distribution system. In: *Power and energy conference, 2004. PECon 2004. Proceedings. National. IEEE*, pp 104–108
- Lascu C, Asiminoaei L, Boldea I, Blaabjerg F (2007) High performance current controller for selective harmonic compensation in active power filters. *IEEE Trans Power Electron* 22:1826–1835
- Lascu C, Asiminoaei L, Boldea I, Blaabjerg F (2009) Frequency response analysis of current controllers for selective harmonic compensation in active power filters. *IEEE Trans Ind Electron* 56:337–347
- Limongi L, Bojoi IR, Griva GB, Tenconi A (2009) Digital current-control schemes. *IEEE Ind Electron Mag* 3:20–31
- Malesani L, Mattavelli P, Buso S (1998) Robust dead-beat current control for PWM rectifiers and active filters. In: *Industry applications conference, 1998. Thirty-third IAS annual meeting. The 1998 IEEE. IEEE*, pp 1377–1384
- Mattavelli P (2001) A closed-loop selective harmonic compensation for active filters. *IEEE Trans Ind Appl* 37:81–89
- Mesbahi N, Ouari A, Abdeslam DO, Djamah T, Omeiri A (2014) Direct power control of shunt active filter using high selectivity filter (HSF) under distorted or unbalanced conditions. *Electr Power Syst Res* 108:113–123
- Noguchi T, Tomiki H, Kondo S, Takahashi I (1998) Direct power control of PWM converter without power-source voltage sensors. *IEEE Trans Ind Appl* 34:473–479
- Rahmani S, Mendalek N, Al-Haddad K (2010) Experimental design of a nonlinear control technique for three-phase shunt active power filter. *IEEE Trans Ind Electron* 57:3364–3375
- Routimo M, Salo M, Tuusa H (2007) Comparison of voltage-source and current-source shunt active power filters. *IEEE Trans Power Electron* 22:636–643
- Shyu K-K, Yang M-J, Chen Y-M, Lin Y-F (2008) Model reference adaptive control design for a shunt active-power-filter system. *IEEE Trans Ind Electron* 55:97–106
- Singh B, Al-Haddad K, Chandra A (1999) A review of active filters for power quality improvement. *IEEE Trans Ind Electron* 46:960–971
- Soares V, Verdelho P, Marques GD (2000) An instantaneous active and reactive current component method for active filters. *IEEE Trans Power Electron* 15:660–669
- Takahashi I, Noguchi T (1986) A new quick-response and high-efficiency control strategy of an induction motor. *IEEE Trans Ind Appl* 5:820–827
- Zhang Y, Xie W, Li Z, Zhang Y (2013) Model predictive direct power control of a PWM rectifier with duty cycle optimization. *IEEE Trans Power Electron* 28:5343–5351